

Dynamics and cosmological constraints on Brans-Dicke cosmology

Orest Hrycyna*

Theoretical Physics Division, National Centre for Nuclear Research, Hoża 69, 00-681 Warszawa, Poland

Michał Kamionka†

Astronomical Institute, University of Wrocław, Kopernika 11, 51-622 Wrocław, Poland

Marek Szydłowski‡

*Astronomical Observatory, Jagiellonian University, Orla 171, 30-244 Kraków, Poland and
Mark Kac Complex Systems Research Centre, Jagiellonian University, Reymonta 4, 30-059 Kraków, Poland
(Dated: June 8, 2019)*

We investigate observational constraints on Brans-Dicke cosmological model using observational data coming from distant supernovae type Ia, the Hubble function $H(z)$ measurements, information coming from Alcock-Paczyński test and baryon acoustic oscillations (BAO). Our analysis is based on modified Friedmann function resulting from dynamical investigations of Brans-Dicke cosmology in vicinity of de Sitter state. Qualitative theory of dynamical systems enables us to obtain three different behaviors in vicinity of this state. We find : for a linear approach to the de Sitter state $\omega_{BD} = -0.8681^{+0.1407}_{-0.0948}$ with the best fit value $\omega_{BD} = -0.9782$, while for an oscillatory approach to the de Sitter state we obtain $\omega_{BD} = -1.2219^{+0.1478}_{-0.0450}$ with the best fit value $\omega_{BD} = -1.0646$, while for the transient de Sitter state represented by a saddle type critical point we find $\omega_{BD} = -1.9499^{+0.0988}_{-0.6576}$ with the best fit value $\omega_{BD} = -1.7817$. We obtain mass of the Brans-Dicke scalar field at the present epoch as $m_\phi \sim H_0$.

PACS numbers: 04.50.Kd, 98.80.-k, 95.36.+x, 95.35.+d

Keywords: modified theories of gravity, cosmology, dark energy, dark matter

I. INTRODUCTION

Composing the standard cosmological model (Λ CDM model) we assume that the general relativity describes universe and we postulate validity of the cosmological principle. This model is the best description of the current universe as indicated by implementing the Bayesian methods of model selection to simple theoretical models [1]. Attempts to explain the present universe in terms of the standard cosmological model is justified by a pragmatic approach of a simple two parameter model. Such a model corresponds to what in physics we know as effective theories, like a standard model in particle physics. In this model as well as in Λ CDM model there are parameters which value should be obtained from a more fundamental theory or determined by observations. In cosmology the role of such parameters play the density parameters. Unfortunately, the nature of some parameters describing dark side of the universe (dark energy and dark matter) is unknown. Adopting the methodology of an effective theory can shed some light on the nature of parameters revealing hints toward a more fundamental theory which we are looking for.

Because of well known problems with the cosmological term in the standard cosmological model related with its substantial interpretation we are looking for solution of

conundrum of acceleration of the current Universe in the framework of Brans-Dicke theory of gravity [2] (see also [3]). In this theory gravitational interaction is described in terms of both the scalar field and the metric.

Our point of view is that in the construction of the standard cosmological model the cosmological constant term plays the role of a useful fiction which is successful in the description but without the explanation, i.e. the Λ CDM model describes cosmological observations but explains nothing. Moreover following recent Planck observations the time varying equation of state with the constant additive contribution is favored when the astrophysical data are taken into account [4].

A scalar field plays an important role in description of the early universe (inflation) as well as the late time cosmic evolution (quintessence). In the cosmological investigations it is explored in the context of obtaining a time-varying form of equation of state. In all these applications the scalar field is treated as a source. Usually it is assumed that they are not free and interact with itself via some potential function. The main problem in scalar field cosmology is that the form of this potential is unknown. Of course in cosmological investigations different forms are assumed a priori in calculations but we do not know which potential for the scalar field ?

In the Brans-Dicke theory, which is a scalar-tensor theory of gravity, a scalar field does not play the role of a substance but is rather a integral part of the gravitational sector description. In this description appears a free parameter ω_{BD} of the theory which is the consequence of the effective theory approach.

* orest.hrycyna@fuw.edu.pl

† kamionka@astro.uni.wroc.pl

‡ marek.szydowski@uj.edu.pl

The value of this parameter can be constrained from different data. In the solar system for spherically symmetric solutions the Cassini spacecraft mission in the parametrized post-Newtonian (PPN) formalism gave very stringent experimental bounds $\omega_{\text{BD}} > 40000$ on the value of the Brans-Dicke parameter [5–7]. From the other approach number of constraints on ω_{BD} parameter have been derived since WMAP and the Planck missions. Recently Avilez and Scordis, using CMB data, gave a lower limit on the ω_{BD} parameter to $\omega_{\text{BD}} > 177$ at 95% confidence level [8]. Li et al. [9] using data coming from the Planck satellite and others cosmological observations excluded ω_{BD} parameter region $-407.0 < \omega_{\text{BD}} < 175.87$ at 95% confidence level, while for positive values of this parameter they obtained $\omega_{\text{BD}} > 181.65$ at 95% confidence level. From the other hand Fabris et al. in [10] using the supernovae Ia data obtained the best fit value of $\omega_{\text{BD}} = -1.477$. We must remember that all these limits are model dependent. In some estimations the potential of the scalar field is ignored while in others the Newtonian approximation and spherical symmetry is assumed at the starting point.

In our methodology we find observational constraints on the Brans-Dicke cosmological model assuming the Robertson-Walker symmetry working at the cosmological scale. Therefore the $H^2(a)$ relation is starting point of our further estimations of the model parameters. The parameter ω_{BD} is hidden behind the density parameters of the cosmological Brans-Dicke modification of the Friedmann equation. The next step is to estimate the value of density parameters from the astronomical data and compare the model with the standard cosmological model Λ CDM using information criteria. Because we treat the new model as a generalization of the Λ CDM model it is naturally to interpret prime contribution to the $H^2(a)$ relation as a corresponding to the Λ CDM model.

The action for the Brans-Dicke theory [2] in so-called Jordan frame is in the following form [11, 12]

$$S = \int d^4x \sqrt{-g} \left(\phi R - \frac{\omega_{\text{BD}}}{\phi} \nabla^\alpha \phi \nabla_\alpha \phi - 2V(\phi) \right) + 16\pi S_m, \quad (1)$$

where the barotropic matter is described by

$$S_m = \int d^4x \sqrt{-g} \mathcal{L}_m, \quad (2)$$

and ω_{BD} is a dimensionless parameter of the theory.

For the spatially flat Friedmann-Robertson-Walker metric field equations lead to the energy conservation condition

$$3H^2 = \frac{\omega_{\text{BD}}}{2} \frac{\dot{\phi}^2}{\phi^2} + \frac{V(\phi)}{\phi} - 3H \frac{\dot{\phi}}{\phi} + \frac{8\pi}{\phi} \rho_m, \quad (3)$$

and the acceleration equation

$$\begin{aligned} \dot{H} = & -\frac{\omega_{\text{BD}}}{2} \frac{\dot{\phi}^2}{\phi^2} - \frac{1}{3+2\omega_{\text{BD}}} \frac{2V(\phi) - \phi V'(\phi)}{\phi} + \\ & + 2H \frac{\dot{\phi}}{\phi} - \frac{8\pi}{\phi} \rho_m \frac{2 + \omega_{\text{BD}}(1 + w_m)}{3 + 2\omega_{\text{BD}}}, \end{aligned} \quad (4)$$

while the equation of motion for the scalar field is in the following form

$$\ddot{\phi} + 3H\dot{\phi} = 2 \frac{2V(\phi) - \phi V'(\phi)}{3 + 2\omega_{\text{BD}}} + 8\pi \rho_m \frac{1 - 3w_m}{3 + 2\omega_{\text{BD}}}. \quad (5)$$

II. DYNAMICS AND THE HUBBLE FUNCTION

Using the expansion normalized variables [13, 14]

$$x \equiv \frac{\dot{\phi}}{H\phi}, \quad y \equiv \sqrt{\frac{V(\phi)}{3\phi}} \frac{1}{H}, \quad \lambda \equiv -\phi \frac{V'(\phi)}{V(\phi)}, \quad (6)$$

the energy conservation condition (3) can be presented as

$$\Omega_m = \frac{8\pi \rho_m}{3\phi H^2} = 1 + x - \frac{\omega_{\text{BD}}}{6} x^2 - y^2, \quad (7)$$

and the acceleration equation (4) as

$$\begin{aligned} \frac{\dot{H}}{H^2} = & 2x - \frac{\omega_{\text{BD}}}{2} x^2 - \frac{3}{3 + 2\omega_{\text{BD}}} y^2 (2 + \lambda) - \\ & - 3 \left(1 + x - \frac{\omega_{\text{BD}}}{6} x^2 - y^2 \right) \frac{2 + \omega_{\text{BD}}(1 + w_m)}{3 + 2\omega_{\text{BD}}}. \end{aligned} \quad (8)$$

Then the dynamics of the Brans-Dicke theory with an arbitrary potential function and the barotropic matter content can be reduced to a 3-dimensional autonomous dynamical system

$$\begin{aligned} \frac{dx}{d\tau} = & -3x - x^2 - x \frac{\dot{H}}{H^2} + \frac{6}{3 + 2\omega_{\text{BD}}} y^2 (2 + \lambda) + \\ & + 3 \left(1 + x - \frac{\omega_{\text{BD}}}{6} x^2 - y^2 \right) \frac{1 - 3w_m}{3 + 2\omega_{\text{BD}}}, \end{aligned} \quad (9a)$$

$$\frac{dy}{d\tau} = -y \left(\frac{1}{2} x (1 + \lambda) + \frac{\dot{H}}{H^2} \right), \quad (9b)$$

$$\frac{d\lambda}{d\tau} = x\lambda (1 - \lambda(\Gamma - 1)), \quad (9c)$$

where $\frac{d}{d\tau} = \frac{d}{d \ln a}$ and

$$\Gamma = \frac{V''(\phi)V(\phi)}{V'(\phi)^2}, \quad (10)$$

where $()' = \frac{d}{d\phi}$.

If we assume that $\Gamma = \Gamma(\lambda)$ we are able to find critical points of the system (9) which depend on the explicit form of the $\Gamma(\lambda)$ function. In our previous paper [13] we have found that for an arbitrary potential function of the scalar field which can be expressed by some $\Gamma(\lambda)$ function, there exist a single critical point ($x^* = 0$, $y^* = 1$, $\lambda^* = -2$) corresponding the de Sitter expansion.

Qualitative behavior of the solutions of the system (9) in the vicinity of this critical point depend on the eigenvalues of the linearization matrix calculated at this point.

The eigenvalues are

$$\begin{aligned} l_1 &= -3(1 + w_m), \\ l_{2,3} &= -\frac{3}{2} \left(1 \pm \sqrt{\frac{3 + 2\omega_{\text{BD}} + \delta}{3 + 2\omega_{\text{BD}}}} \right), \end{aligned} \quad (11)$$

where δ parameter is defined as

$$\delta = \frac{8}{3} \lambda^* (1 - \lambda^* (\Gamma(\lambda^*) - 1)) = \frac{16}{3} (1 - 2\Gamma^*), \quad (12)$$

and depends on the second derivative of the potential function at the de Sitter state. Note that for a quadratic potential function $V(\phi) \propto \phi^2$ we have $\Gamma = \frac{1}{2}$ which leads to $\delta = 0$. Simple inspection of the eigenvalues gives that in this case one of them vanishes giving rise to degenerated critical point and structurally unstable system [14, 15].

For $w_m > -1$ the critical point corresponding to the de Sitter expansion is stable when $\frac{\delta}{3+2\omega_{\text{BD}}} < 0$ and represents a saddle type critical point otherwise. The stable case can be further divided in to two cases corresponding to a stable node for $-1 < \frac{\delta}{3+2\omega_{\text{BD}}} < 0$ and a stable focus for $\frac{\delta}{3+2\omega_{\text{BD}}} < -1$. In the most general case, from

(11), one can distinguish two cases, the first one when the eigenvalues of the linearization matrix are purely real and the second when the eigenvalues have a non-zero imaginary part. The case with purely imaginary eigenvalues is excluded in our case.

From now on we assume that we include only the baryonic matter, $\Omega_m = \Omega_{bm}$ with the equation of state parameter $w_m = 0$.

In Appendix A we presented the linearized solutions in the vicinity of the de Sitter state for two types of behavior.

The first case, characterized by the purely real eigenvalues, we make the following substitution

$$\frac{\delta}{3 + 2\omega_{\text{BD}}} = \frac{4}{9} n(n - 3), \quad (13)$$

and the eigenvalues of the linearization matrix at the de Sitter state are

$$l_1 = -3, \quad l_2 = -n, \quad l_3 = -3 + n, \quad (14)$$

where for $0 < n < \frac{3}{2}$ we have a stable node critical point and for $n < 0$ a saddle type. Now, using the linearized solutions (A3) and the acceleration equation (8) up to linear terms in initial conditions we obtain the following Hubble function

$$\left(\frac{H(a)}{H(a_0)} \right)^2 = \Omega_{\Lambda,0} + \Omega_{M,0} \left(\frac{a}{a_0} \right)^{-3} + \Omega_{n,0} \left(\frac{a}{a_0} \right)^{-n} + \Omega_{3n,0} \left(\frac{a}{a_0} \right)^{-3+n}, \quad (15)$$

where

$$\Omega_{M,0} = \left(1 - \frac{16}{3\delta} \right) \Omega_{bm,0}, \quad (16a)$$

$$\Omega_{n,0} = \frac{n+1}{3\delta(2n-3)} \left(4n \Omega_{bm,i} - 3\delta \Delta x + 8(n-3)\Delta\lambda \right) \left(\frac{a_0}{a^{(i)}} \right)^{-n}, \quad (16b)$$

$$\Omega_{3n,0} = \frac{n-4}{3\delta(2n-3)} \left(-4(n-3) \Omega_{bm,i} - 3\delta \Delta x - 8n\Delta\lambda \right) \left(\frac{a_0}{a^{(i)}} \right)^{-3+n}, \quad (16c)$$

and

$$\Omega_{\Lambda,0} = 1 - \Omega_{M,0} - \Omega_{n,0} - \Omega_{3n,0}. \quad (17)$$

In our further investigation the model described by the Hubble function (15) together with $0 < n < \frac{3}{2}$ we denote as “model 1a” (the de Sitter state is the critical point of a stable node type), while the model with $n < 0$ we denote as “model 1b” (the de Sitter state is a saddle type critical point).

For the second type of behavior in the vicinity of the de Sitter state we make the following substitution

$$\frac{\delta}{3 + 2\omega_{\text{BD}}} = -\frac{1}{9} (9 + 4n^2), \quad (18)$$

and the eigenvalues of the linearization matrix at the de Sitter state are

$$l_1 = -3, \quad l_2 = -\frac{3}{2} - \mathfrak{i}n, \quad l_3 = -\frac{3}{2} + \mathfrak{i}n. \quad (19)$$

From the solutions (A6) and the acceleration equation (8), and again, up to linear terms in initial conditions we obtain the following Hubble function

$$\left(\frac{H(a)}{H(a_0)}\right)^2 = \Omega_{\Lambda,0} + \Omega_{M,0} \left(\frac{a}{a_0}\right)^{-3} + \left(\frac{a}{a_0}\right)^{-3/2} \left(\Omega_{cos,0} \cos\left(n \ln\left(\frac{a}{a_0}\right)\right) + \Omega_{sin,0} \sin\left(n \ln\left(\frac{a}{a_0}\right)\right) \right), \quad (20)$$

where

$$\Omega_{M,0} = \left(1 - \frac{16}{3\delta}\right) \Omega_{bm,0}, \quad (21a)$$

$$\Omega_{cos,0} = \frac{1}{3\delta} \left(16 \Omega_{bm,i} - 3\delta \Delta x + 8\Delta\lambda\right) \left(\frac{a_0}{a^{(i)}}\right)^{-3/2} \cos\left(n \ln\left(\frac{a_0}{a^{(i)}}\right)\right) + \frac{1}{6\delta n} \left(2(4n^2 - 15) \Omega_{bm,i} + 15\delta \Delta x + 4(4n^2 + 15)\Delta\lambda\right) \left(\frac{a_0}{a^{(i)}}\right)^{-3/2} \sin\left(n \ln\left(\frac{a_0}{a^{(i)}}\right)\right), \quad (21b)$$

$$\Omega_{sin,0} = \frac{1}{6\delta n} \left(2(4n^2 - 15) \Omega_{bm,i} + 15\delta \Delta x + 4(4n^2 + 15)\Delta\lambda\right) \left(\frac{a_0}{a^{(i)}}\right)^{-3/2} \cos\left(n \ln\left(\frac{a_0}{a^{(i)}}\right)\right) - \frac{1}{3\delta} \left(16 \Omega_{bm,i} - 3\delta \Delta x + 8\Delta\lambda\right) \left(\frac{a_0}{a^{(i)}}\right)^{-3/2} \sin\left(n \ln\left(\frac{a_0}{a^{(i)}}\right)\right). \quad (21c)$$

and

$$\Omega_{\Lambda,0} = 1 - \Omega_{M,0} - \Omega_{cos,0} \quad (22)$$

The model described by the Hubble function (20) we denote as “model 2” (the de Sitter state corresponds to the critical point of a stable focus type).

Note that for the Hubble functions (15) and (20), when the parameter δ in (16a) and (21a) is negative $\delta < 0$, the density parameter of the matter content $\Omega_{M,0}$ is larger than the density parameter of the matter included in the model by hand $\Omega_{bm,0}$.

Additionally the Λ CDM model is nested within both Hubble functions (15) and (20), i.e. carefully choosing the initial conditions for the linearized solutions

$$\Delta x = \frac{4}{\delta} \Omega_{bm,i}, \quad \Delta\lambda = -\frac{1}{2} \Omega_{bm,i}, \quad (23)$$

where up to linear terms in initial conditions $\Omega_{bm,i} = \Delta x - 2\Delta y$, then in (15) we have $\Omega_{n,0} = \Omega_{3n,0} = 0$ and in (20) we have $\Omega_{cos,0} = \Omega_{sin,0} = 0$ and the resulting form of the Hubble function is

$$\left(\frac{H(a)}{H(a_0)}\right)^2 \approx 1 - \Omega_{M,0} + \Omega_{M,0} \left(\frac{a}{a_0}\right)^{-3}, \quad (24)$$

where

$$\Omega_{M,0} = \left(1 - \frac{16}{3\delta}\right) \Omega_{bm,0}. \quad (25)$$

This Hubble function describes the Λ CDM model with direct interpretation of the second term in the brackets as proportional to density parameter of the dark matter in the model

$$\Omega_{dm,0} = -\frac{16}{3\delta} \Omega_{bm,0}. \quad (26)$$

III. OBSERVATIONAL CONSTRAINS

To estimate the parameters of the models we used modified for our purposes, publicly available COSMOMC source code [16, 17] with implemented nested sampling algorithm MULTINEST [18–20]. We kept fixed present values of the Hubble function $H_0 = 67.4$ Mpc/km/s and the baryonic matter density parameter $\Omega_{bm,0} h^2 = 0.02207$ taken for the recent observations of the Planck satellite [4]. In all investigated models we assumed a flat prior for estimated parameters in the following intervals: $\Omega_{M,0} \in (0.1; 0.5)$, $\Omega_{n,0} \in (-0.25; 0.25)$, $\Omega_{3n,0} \in (0.25; 0.25)$ and the parameter n for the model 1a $n \in (0; \frac{3}{2})$ and for the model 1b $n \in (-3; 0)$. For the model 2 we assumed $\Omega_{sin,0} \in (-0.25; 0.25)$, $\Omega_{cos,0} \in (-0.25; 0.25)$ and $n \in (0; 5)$.

We used observational data of 580 supernovae type Ia – so called UNION2.1 compilation [21], 31 observational data points of Hubble function from [22–31] collected in [32], the measurements of BAO (baryon acoustic oscillations) from Sloan Digital Sky Survey (SDSS-III) combined with 2dF Galaxy Redshift Survey (2dFGRS) [33–36], The 6dF Galaxy Survey (6dFGS) [37, 38], WiggleZ Dark Energy Survey [39–41] and information coming from determinations of Hubble function using Alcock–Paczynski test [42, 43].

The likelihood function for the supernovae data is defined by:

$$L_{SN} \propto \exp \left[- \sum_{i,j} (\mu_i^{\text{obs}} - \mu_i^{\text{th}}) \mathbb{C}_{ij}^{-1} (\mu_j^{\text{obs}} - \mu_j^{\text{th}}) \right], \quad (27)$$

where \mathbb{C}_{ij} is the covariance matrix with the systematic errors, $\mu_i^{\text{obs}} = m_i - M$ is the distance modulus, $\mu_i^{\text{th}} =$

$5 \log_{10} D_{Li} + \mathcal{M} = 5 \log_{10} d_{Li} + 25$, $\mathcal{M} = -5 \log_{10} H_0 + 25$ and $D_{Li} = H_0 d_{Li}$, where d_{Li} is the luminosity distance which is given by $d_{Li} = (1 + z_i) c \int_0^{z_i} \frac{dz'}{H(z')}$ (with the assumption $k = 0$).

For $H(z)$ the likelihood function is given by:

$$L_{H(z)} \propto \exp \left[- \sum_i \frac{(H^{\text{th}}(z_i) - H_i^{\text{obs}})^2}{2\sigma_i^2} \right], \quad (28)$$

where $H^{\text{th}}(z_i)$ denotes the theoretically estimated Hubble function, H_i^{obs} is observational data.

For BAO A parameter the likelihood function is defined as:

$$L_{BAOA} \propto \exp \left[- \sum_{i,j} (A^{\text{th}}(z_i) - A_i^{\text{obs}}) \mathbb{C}_{ij}^{-1} (A^{\text{th}}(z_j) - A_j^{\text{obs}}) \right], \quad (29)$$

where: \mathbb{C}_{ij} is the covariance matrix with the systematic errors, $A^{\text{th}}(z_i) = \sqrt{\Omega_{m,0}} \left(\frac{H(z_i)}{H_0} \right)^{-\frac{1}{3}} \left[\frac{1}{z_i} \int_0^{z_i} \frac{H_0}{H(z)} dz \right]^{\frac{2}{3}}$.

The likelihood function for the rest of BAO data is characterized by:

$$L_{BAO} \propto \exp \left[- \sum_{i,j} (d^{\text{th}}(z_i) - d_i^{\text{obs}}) \mathbb{C}_{ij}^{-1} (d^{\text{th}}(z_j) - d_j^{\text{obs}}) \right], \quad (30)$$

where: \mathbb{C}_{ij} is the covariance matrix with the systematic errors, $d^{\text{th}}(z_i) \equiv r_s(z_d) \left[(1 + z_i)^2 D_A^2(z_i) \frac{cz_i}{H(z_i)} \right]^{-\frac{1}{3}}$, $r_s(z_d)$ is the sound horizon at the drag epoch and D_A is the angular diameter distance.

And finally, the likelihood function for the information coming from Alcock-Paczynski test is given by:

$$L_{AP} \propto \exp \left[- \sum_i \frac{(AP^{\text{th}}(z_i) - AP_i^{\text{obs}})^2}{2\sigma_i^2} \right], \quad (31)$$

where: $AP^{\text{th}}(z_i) \equiv \frac{H(z_i)}{H_0(1+z_i)}$.

The total likelihood function L_{TOT} is defined as:

$$L_{TOT} = L_{SN} L_{H(z)} L_{BAOA} L_{BAO} L_{AP}. \quad (32)$$

The mean of marginalized posterior PDF with 68% confidence level together with values of the joined posterior probabilities of the parameters for all investigated models are gathered in Table I.

The posterior constraints for investigated models are given at Figs. 1, 2 and 3. On the one dimensional plots the solid lines denote fully marginalized probabilities and the dotted lines show mean likelihood. On the two dimensional plots the solid lines denote 68% and 95% credible intervals of fully marginalized probabilities while the colors illustrate mean likelihood of the sample used.

We used BIC quantity [44] as an approximation which is proportional to the evidence and is defined as

$$BIC = -2 \ln \mathcal{L} + d \ln N, \quad (33)$$

TABLE I. Mean of marginalized posterior PDF with 68% confidence level for the parameters of the models. In the brackets are shown parameter's values of joined posterior probabilities. Estimations were made using *Union2.1*, $H(z)$, *Alcock-Paczynski* and *BAO* data sets.

	<i>Union2.1</i> + $H(z)$ + <i>AP</i>	<i>Union2.1</i> + $H(z)$ + <i>AP</i> + <i>BAO</i>
model 1a		
$\Omega_{M,0}$	$0.2688_{-0.0275}^{+0.0276}$ (0.2876)	$0.3009_{-0.0054}^{+0.0047}$ (0.3030)
$\Omega_{n,0}$	$0.0159_{-0.0775}^{+0.0850}$ (0.1682)	$0.0586_{-0.0579}^{+0.0804}$ (0.1875)
$\Omega_{3n,0}$	$0.0533_{-0.0548}^{+0.0678}$ (-0.0558)	$-0.0168_{-0.0173}^{+0.0206}$ (-0.1189)
n	$0.6810_{-0.2854}^{+0.2390}$ (1.2756)	$0.8504_{-0.2003}^{+0.2771}$ (1.2670)
model 1b		
$\Omega_{M,0}$	$0.3278_{-0.0407}^{+0.0486}$ (0.2656)	$0.3069_{-0.0078}^{+0.0078}$ (0.3085)
$\Omega_{n,0}$	$-0.0107_{-0.0887}^{+0.0818}$ (-0.1793)	$-0.0404_{-0.0743}^{+0.0568}$ (-0.1428)
$\Omega_{3n,0}$	$-0.0186_{-0.0278}^{+0.0228}$ (0.0019)	$-0.0056_{-0.0040}^{+0.0048}$ (-0.0068)
n	$-0.5236_{-0.0544}^{+0.2984}$ (-1.8458)	$-0.6813_{-0.1360}^{+0.3648}$ (-1.0046)
model 2		
$\Omega_{M,0}$	$0.2917_{-0.0158}^{+0.0154}$ (0.2782)	$0.3036_{-0.0060}^{+0.0051}$ (0.3051)
$\Omega_{cos,0}$	$0.0430_{-0.0547}^{+0.0634}$ (0.0836)	$0.0653_{-0.0419}^{+0.0337}$ (0.1271)
$\Omega_{sin,0}$	$-0.0119_{-0.0561}^{+0.0531}$ (-0.0138)	$0.0388_{-0.0466}^{+0.0375}$ (0.1929)
n	$1.3912_{-0.6491}^{+0.2901}$ (0.2646)	$1.3642_{-0.6576}^{+0.2351}$ (0.5999)
Λ CDM model		
$\Omega_{M,0}$	$0.2995_{-0.0021}^{+0.0021}$ (0.2993)	$0.3001_{-0.0019}^{+0.0019}$ (0.3003)

where \mathcal{L} is the maximum of the likelihood function, d is the number of model parameters and N is the number of the data points.

We use also the Bayes factor

$$B_{0i} = \frac{E_0}{E_i} \quad (34)$$

which is the ratio of the evidence of the base model E_0 and the model investigated E_i . The logarithm of evidence has an asymptotic approximation

$$\ln E = \ln \mathcal{L} - \frac{d}{2} \ln N, \quad (35)$$

which can be directly connected with the value of the BIC quantity as

$$E_i = \exp \left(-\frac{1}{2} BIC_i \right). \quad (36)$$

TABLE II. Values of χ^2 , BIC and the Bayes factor (with respect to Λ CDM model) for *Union2.1+H(z)+Alcock-Paczynski* and *Union2.1+H(z)+Alcock-Paczynski+BAO* data sets.

<i>Union2+H(z)+AP</i>			
	$\chi^2/2$	<i>BIC</i>	$2 \ln B_{0i}$
model 1a	282.7862	591.2589	12.4754
model 1b	282.7209	591.1283	12.3448
model 2	282.7843	591.2551	12.4717
Λ CDM	282.9701	578.7834	0
<i>Union2+H(z)+AP+BAO</i>			
	$\chi^2/2$	<i>BIC</i>	$2 \ln B_{0i}$
model 1a	282.7791	591.2836	12.4713
model 1b	282.7388	591.2029	12.3907
model 2	282.7623	591.2499	12.4377
Λ CDM	282.9748	578.8122	0

Thus we obtain that twice of the natural logarithm of the Bayes factor of two models as

$$2 \ln B_{0i} = \frac{1}{2} (BIC_i - BIC_0). \quad (37)$$

This quantity can be interpreted as a evidence in favor of the base model with subscript “0”. For $2 > 2 \ln B_{0i} > 0$ the evidence is not worth a bare mention, for $6 > 2 \ln B_{0i} > 2$ is positive, for $10 > 2 \ln B_{0i} > 6$ is strong and when $2 \ln B_{0i} > 10$ the evidence is very strong in favor of model “0” (or very strong evidence against model “i”) [45].

The values of twice the natural logarithm of the Bayes factor of models 1a, 1b and 2 with respect to the Λ CDM model are gathered in Table II. These values are greater than 10 indicating that there are strong evidence against three models considered as compared to the Λ CDM model (or, equivalently, the strong evidence in favor of the Λ CDM as compared to the three models considered).

Calculating twice the natural logarithm of the Bayes factor between the models under investigations we obtain, for models 1a and 1b : $2 \ln B_{1a1b} = 0.0403$, for models 1a and 2 : $2 \ln B_{1a2} = 0.0235$ and for models 2 and 1b : $2 \ln B_{21b} = 0.0169$. These values are smaller than 2 and the comparison between proposed models do not favor neither of them.

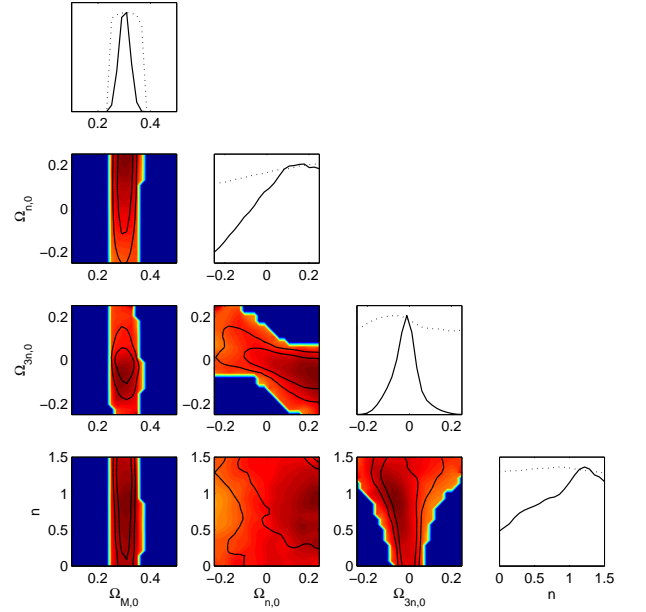


FIG. 1. Posterior constraints for investigated model 1a (linear approach to the de Sitter state). 1D plots: solid lines denote fully marginalized probabilities, dotted lines show mean likelihood. 2D plots: solid lines denote 68 % and 95 % credible intervals of fully marginalized probabilities, the colors illustrate mean likelihood of the sample. Estimations were made using *Union2.1+H(z)+Alcock-Paczynski+BAO* data set. For the numerical results see Table I.

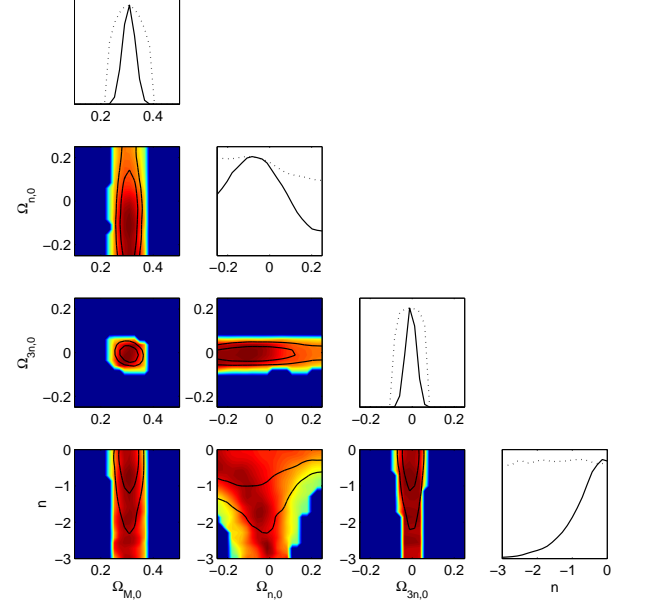


FIG. 2. Posterior constraints for investigated model 1b (transient de Sitter evolution). 1D plots: solid lines denote fully marginalized probabilities, dotted lines show mean likelihood. 2D plots: solid lines denote 68 % and 95 % credible intervals of fully marginalized probabilities, the colors illustrate mean likelihood of the sample. Estimations were made using *Union2.1+H(z)+Alcock-Paczynski+BAO* data set. For the numerical results see Table I.

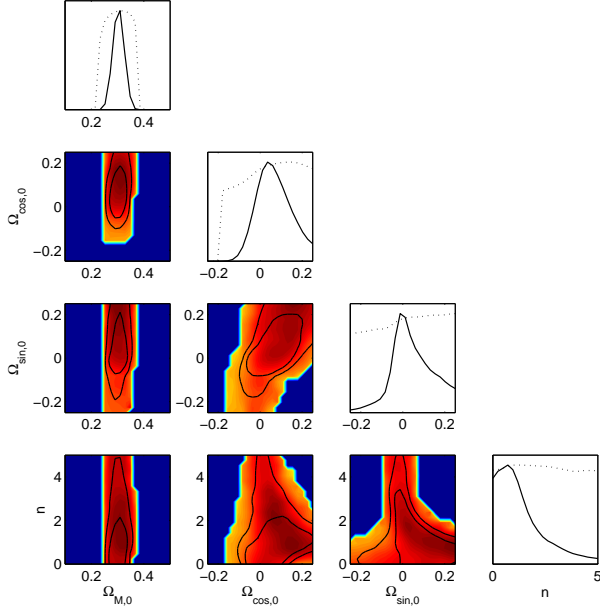


FIG. 3. Posterior constraints for investigated model 2 (oscillatory approach to the de Sitter state). 1D plots: solid lines denote fully marginalized probabilities, dotted lines show mean likelihood. 2D plots: solid lines denote 68 % and 95 % credible intervals of fully marginalized probabilities, the colors illustrate mean likelihood of the sample. Estimations were made using *Union2.1+H(z)+Alcock-Paczynski+BAO* data set. For the numerical results see Table I.

IV. DERIVED QUANTITIES

In the previous section we have estimated values of the unknown parameters of the models. The two pairs of parameters $(\Omega_{n,0}, \Omega_{3n,0})$ and $(\Omega_{sin,0}, \Omega_{cos,0})$ depend on the initial conditions of the phase space variables. Knowing the values of the parameters of the models one is able to obtain complete information about the present state of the phase space variables.

The action integral (1) gives the effective gravitational coupling in Brans-Dicke theory as an inverse of the scalar field

$$G_{\text{eff}} = \frac{1}{\phi}. \quad (38)$$

However, for the spherically symmetric solutions in the Brans-Dicke theory in Cavendish-like experiments we have [46–48]

$$G_{\text{eff}} = \frac{1}{\phi} \frac{4 + 2\omega_{\text{BD}}}{3 + 2\omega_{\text{BD}}}. \quad (39)$$

We have to remember that this quantity is defined in the context of the parametrized post-Newtonian (PPN) formalism [5] only suitable for the solar system tests where

a spherical symmetry of solutions is assumed, and not for cosmological considerations [11].

The variation of the effective gravitational coupling in the Brans-Dicke theory can be directly connected with the cosmological evolution of the scalar field

$$\frac{\dot{G}_{\text{eff}}}{G_{\text{eff}}} = -\frac{\dot{\phi}}{\phi}. \quad (40)$$

Thus we have a direct interpretation of the present value of the phase space variable x

$$x(a_0) = \frac{\dot{\phi}}{H\phi} \Big|_0 = -\frac{\dot{G}}{HG} \Big|_0, \quad (41)$$

where in G we omitted the subscript for simplicity. For the remaining two of the phase space variables we have

$$y(a_0) = \sqrt{\frac{V(\phi_0)}{3\phi_0}} \frac{1}{H_0}, \quad \lambda(a_0) = -\phi_0 \frac{V'(\phi_0)}{V(\phi_0)}, \quad (42)$$

where the first quantity is proportional to the value of the scalar field potential function at the present epoch and the second one gives the slope of the potential function at the present epoch.

The dynamical system analysis enables us to find the asymptotic values of the phase space variables while the linearized solutions give us an opportunity to find its present time values. From equations A3 for the models 1a and 1b we can derive

$$x(a_0) = \frac{3}{4}(\Omega_{bm,0} - \Omega_{M,0}) - \frac{n}{n+1}\Omega_{n,0} - \frac{n-3}{n-4}\Omega_{3n,0}, \quad (43a)$$

$$y(a_0) = 1 - \frac{1}{8}(\Omega_{bm,0} + 3\Omega_{M,0}) - \frac{1}{2}\frac{n}{n+1}\Omega_{n,0} - \frac{1}{2}\frac{n-3}{n-4}\Omega_{3n,0}, \quad (43b)$$

$$\lambda(a_0) = -2 - \frac{1}{2}\Omega_{bm,0} - \frac{3}{8}\frac{1}{n+1}\Omega_{n,0} - \frac{3}{8}\frac{1}{n-4}\Omega_{3n,0}, \quad (43c)$$

while from A6 for the model 2 we find

$$x(a_0) = \frac{3}{4}(\Omega_{bm,0} - \Omega_{M,0}) + \frac{2}{4n^2 + 25}(5\Omega_{cos,0} + 2n\Omega_{sin,0}) - \Omega_{cos,0}, \quad (44a)$$

$$y(a_0) = 1 - \frac{1}{8}(\Omega_{bm,0} + 3\Omega_{M,0}) + \frac{1}{4n^2 + 25}(5\Omega_{cos,0} + 2n\Omega_{sin,0}) - \frac{1}{2}\Omega_{cos,0}, \quad (44b)$$

$$\lambda(a_0) = -2 - \frac{1}{2}\Omega_{bm,0} + \frac{4}{4n^2 + 25} \frac{\Omega_{bm,0}}{\Omega_{bm,0} - \Omega_{M,0}}(5\Omega_{cos,0} + 2n\Omega_{sin,0}). \quad (44c)$$

TABLE III. The present values of the phase space variables $x(a)$, $y(a)$ and $\lambda(a)$ calculated for the mean of marginalized posterior PDF with 68% confidence level for the parameters of the models.

<i>Union2.1+H(z)+AP</i>			
	$x(a_0)$	$y(a_0)$	$\lambda(a_0)$
model 1a	$-0.2088^{+0.0949}_{-0.1072}$	$0.8713^{+0.0474}_{-0.0536}$	$-2.0218^{+0.0267}_{-0.0297}$
model 1b	$-0.2067^{+0.1614}_{-0.1785}$	$0.8723^{+0.0807}_{-0.0892}$	$-2.0174^{+0.0818}_{-0.0738}$
model 2	$-0.2142^{+0.0598}_{-0.0693}$	$0.8686^{+0.0299}_{-0.0347}$	$-2.0287^{+0.0112}_{-0.0142}$
<i>Union2.1+H(z)+AP+BAO</i>			
	$x(a_0)$	$y(a_0)$	$\lambda(a_0)$
model 1a	$-0.2048^{+0.0432}_{-0.0642}$	$0.8733^{+0.0216}_{-0.0321}$	$-2.0382^{+0.0142}_{-0.0215}$
model 1b	$-0.2758^{+0.1687}_{-0.4367}$	$0.8378^{+0.0844}_{-0.2183}$	$-1.9772^{+0.1884}_{-0.0814}$
model 2	$-0.2299^{+0.0402}_{-0.0375}$	$0.8608^{+0.0201}_{-0.0188}$	$-2.0345^{+0.0082}_{-0.0073}$

These equations express the interrelation between the parameters estimated in the Hubble function and the phase space state of the dynamical system under considerations.

In Table III we have gathered the present values of the phase space variables $x(a_0)$, $y(a_0)$ and $\lambda(a_0)$ calculated for the mean of marginalized posterior PDF with 68% confidence level for the parameters of the models. The errors for a given quantity were calculated as minimal and maximal value of the quantity within 1σ intervals of the estimated parameters.

In Fig. 4 we present the fully marginalized probabilities (solid lines) and mean likelihood (dotted lines) for the present value of the phase space variable $x(a_0)$ which is directly connected with time variation of the effective gravitational coupling constant. We have that at present epoch

$$\left. \frac{\dot{G}}{G} \right|_0 = -x(a_0)H_0, \quad (45)$$

which indicates that for every investigated model this quantity is positive, and thus, the value of the effective gravitational coupling constant increases during the evolution of universe. This observation can indicate the weakening the strength of gravity at early times and might be the reason for the low entropy of the early universe [49].

Knowing the present time value of the $y(a_0)$ phase space variable one is able to calculate the scalar field

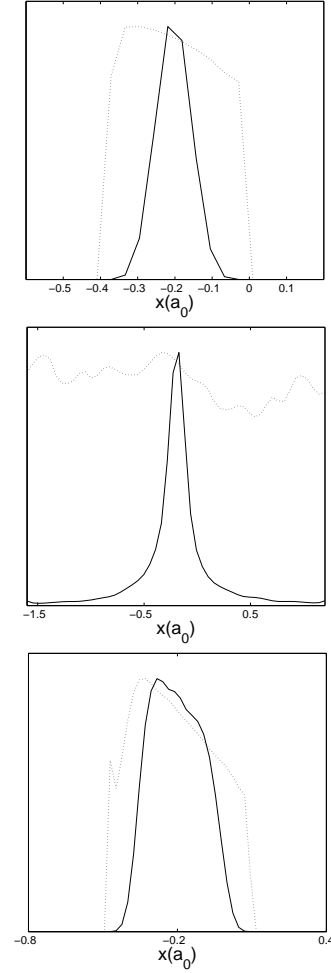


FIG. 4. The fully marginalized probabilities (solid lines) and mean likelihood (dotted lines) for the present value of the phase space variable $x(a_0)$ calculated for the models 1a (top) and 1b (middle) from equation (43a) and for the model 2 (bottom) from equation (44a). The maximal probability is located at the negative values indicating that at present the effective gravitational coupling constant increases.

potential function value at the present time, which is

$$V(\phi_0) = 3\phi_0 H_0^2 (y(a_0))^2. \quad (46)$$

Additionally from the $\lambda(a_0)$ we are able to calculate the first derivative of the scalar field potential function with respect to the scalar field as

$$V'(\phi_0) = -3H_0^2 (y(a_0))^2 \lambda(a_0). \quad (47)$$

The most important parameter in the Brans-Dicke theory is the only free parameter of the theory, namely, ω_{BD} parameter.

TABLE IV. Values of the Brans-Dicke parameter ω_{BD} calculated for the mean of marginalized posterior PDF with 68% confidence level and the best fit parameters of the models.

<i>Union2.1+H(z)+AP</i>		
	ω_{BD}	
	mean	best fit
model 1a	$-0.6618^{+0.6299}_{-0.2236}$	-0.9456
model 1b	$-2.0658^{+0.1358}_{-1.1171}$	-1.6502
model 2	$-1.2135^{+0.1715}_{-0.0644}$	-0.9528
<i>Union2.1+H(z)+AP+BAO</i>		
	ω_{BD}	
	mean	best fit
model 1a	$-0.8681^{+0.1407}_{-0.0948}$	-0.9782
model 1b	$-1.9499^{+0.0988}_{-0.6576}$	-1.7817
model 2	$-1.2219^{+0.1478}_{-0.0450}$	-1.0646

From (16a) and (21a) we obtain that the δ parameter can be directly expressed as

$$\delta = \frac{16\Omega_{bm,0}}{3(\Omega_{bm,0} - \Omega_{M,0})}, \quad (48)$$

where in our considerations $\Omega_{bm,0}$ is the fixed value and $\Omega_{M,0}$ was estimated from the astronomical observational data. Then from (13) we have

$$\omega_{\text{BD}} = -\frac{3}{2} + \frac{6}{n(n-3)} \frac{\Omega_{bm,0}}{\Omega_{bm,0} - \Omega_{M,0}} \quad (49)$$

and from (18) we obtain

$$\omega_{\text{BD}} = -\frac{3}{2} - \frac{24}{9+4n^2} \frac{\Omega_{bm,0}}{\Omega_{bm,0} - \Omega_{M,0}}. \quad (50)$$

Note, that there is only one possibility to obtain $\omega_{\text{BD}} \gg 1$, namely when in (49) the estimated value of n parameter is $n \approx 0$ (or equivalently $n \approx 3$).

In Table IV we gathered the values of the Brans-Dicke parameter ω_{BD} calculated for the mean of marginalized posterior PDF with 68% confidence level and the best fit parameters of the models while on figure 5 we present the fully marginalized probabilities and mean likelihood for the ω_{BD} parameter of the Brans-Dicke theory. In the first case for the model 1a one can notice a clear cutoff at $\omega_{\text{BD}} = -3/2$ as the value leading to pathologies in the model [50].

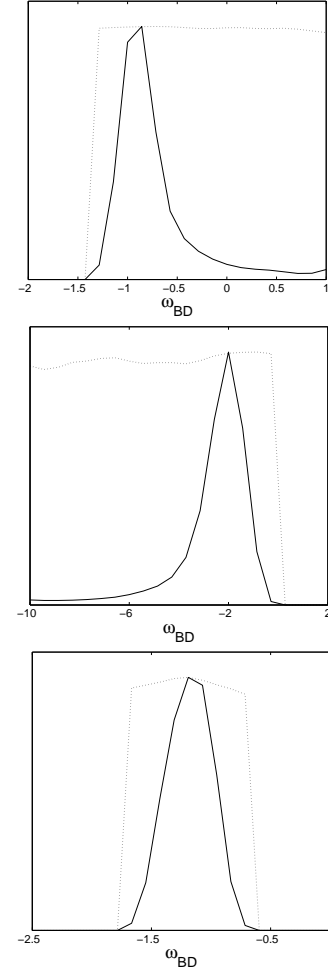


FIG. 5. The fully marginalized probabilities (solid lines) and mean likelihood (dotted lines) for the parameter of the Brans-Dicke theory ω_{BD} calculated for the models 1a (top) and 1b (middle) from equation (49) and for the model 2 (bottom) from equation (50).

Finally we can calculate the mass of the Brans-Dicke scalar field. In the Jordan frame we have [51]

$$m^2 = \frac{2}{3+2\omega_{\text{BD}}} (\phi V''(\phi) - V'(\phi)), \quad (51)$$

which, transformed into the investigated phase space variables, is

$$m^2 = \frac{6}{3+2\omega_{\text{BD}}} H^2 y^2 \lambda (1 + \lambda \Gamma(\lambda)). \quad (52)$$

The mass of the Brans-Dicke scalar field is dynamical quantity and changes during the evolution of universe as well it depends on the form of the scalar field potential function. Using linearized solution to the dynamics one can calculate not only its asymptotic value at the de Sitter state but also its present value.

From the third equation (9c) of the dynamical system (9) describing the evolution of models we obtain that at

the present epoch

$$a \frac{d\lambda}{da} \Big|_0 = x(a_0) \lambda(a_0) \left(1 - \lambda(a_0) (\Gamma(\lambda(a_0)) - 1) \right), \quad (53)$$

and using the linearized solutions (A3) and (A6) one can calculate the quantity on the left hand side of the equation. Then we obtain the present value of the $\Gamma(\lambda(a_0))$ function which depends on the second derivative of the scalar field potential function.

Finally we can express the mass of the Brans-Dicke scalar field at the present epoch as

$$m^2 \Big|_0 = \frac{6}{3 + 2\omega_{\text{BD}}} H(a_0)^2 y(a_0)^2 \times \left((2 + \lambda(a_0)) \lambda(a_0) - \frac{1}{x(a_0)} a_0 \frac{d\lambda}{da} \Big|_0 \right) \quad (54)$$

where from (A3c) and (43c) we have

$$a_0 \frac{d\lambda}{da} \Big|_0 = \frac{3}{2} \Omega_{bm,0} + \frac{3}{8} \frac{n}{n+1} \Omega_{n,0} - \frac{3}{8} \frac{n-3}{n-4} \Omega_{3n,0}, \quad (55)$$

while from (A6c) and (44c) we have

$$a_0 \frac{d\lambda}{da} \Big|_0 = \frac{3}{2} \Omega_{bm,0} + \frac{2}{4n^2 + 25} \frac{\Omega_{bm,0}}{\Omega_{bm,0} - \Omega_{M,0}} \times \left(- (4n^2 + 15) \Omega_{cos,0} + 4n \Omega_{sin,0} \right). \quad (56)$$

For a linear approach to the de Sitter state (model 1a) we obtain the mass of the Brans-Dicke scalar field

$$m^2 \Big|_0 = 1.8249_{-0.5285}^{+0.5622} H_0^2, \quad (57)$$

while for an oscillatory approach to the de Sitter state (model 2) we have the following mass at the present epoch

$$m^2 \Big|_0 = 3.6062_{-1.2367}^{+0.7519} H_0^2. \quad (58)$$

In the model 1b the de Sitter state is represented by a saddle type critical point and we obtain

$$m^2 \Big|_0 = -1.6033_{-2.3057}^{+1.6196} H_0^2. \quad (59)$$

In two first cases we obtain mass of the Brans-Dicke scalar field as

$$m|_0 \sim H_0 \quad (60)$$

which is consistent with an upper bound on the mass of an ultralight pseudo Nambu-Goldstone bosons considered in a cosmological background [52, 53]. In the model 1b where the de Sitter state is a transient state (represented by a saddle type critical point) the mass of the Brans-Dicke scalar field is of a tachyonic type.

V. CONCLUSIONS

In this paper we obtained cosmological constraints on the models resulting from dynamical analysis of the Brans-Dicke theory. We have shown that for an arbitrary potential function of the Brans-Dicke scalar field there exists the de Sitter state and that the dynamical behavior in its vicinity crucially depends on the value of the first and second derivative of the scalar field potential function at the de Sitter state as well as on the value of the Brans-Dicke parameter. We found the following values of the parameter of the theory: for a linear approach to the de Sitter state $\omega_{\text{BD}} = -0.8681_{-0.0948}^{+0.1407}$ with the best fit value $\omega_{\text{BD}} = -0.9782$, while for an oscillatory approach to the de Sitter state we obtain $\omega_{\text{BD}} = -1.2219_{-0.0450}^{+0.1478}$ with the best fit value $\omega_{\text{BD}} = -1.0646$, and for the transient de Sitter state represented by a saddle type critical point we find $\omega_{\text{BD}} = -1.9499_{-0.6576}^{+0.0988}$ with the best fit value $\omega_{\text{BD}} = -1.7817$. It is interesting that for the models under investigation, for an arbitrary scalar field potential function and excluding the model with $\omega_{\text{BD}} < -3/2$ as one leading to ghost behavior, we obtained value of the ω_{BD} parameter close to the value needed to obtain correspondence with the low-energy limit of the bosonic string theory.

Our results show that if we concentrate on generic features of evolution of Brans-Dicke cosmological models then they are represented by a global attractor in the phase space. Using astronomical observational data we estimated density parameters in the Hubble function obtained directly from dynamics of the model. Then from these density parameters we were able to obtain value of the free parameter of the theory ω_{BD} parameter. We shown that the models with the de Sitter state in the form of a saddle type critical point favor the ghost range of the ω_{BD} parameter $\omega_{\text{BD}} < -3/2$. Finally, we shown that in the models with the de Sitter state in the form of a stable node or a sink type critical point values of the ω_{BD} parameter close to the value suggested by the low-energy limit of the bosonic string theory are favored.

ACKNOWLEDGMENTS

We are very grateful to Adam Krawiec for valuable suggestions and comments.

The research of O.H. was supported by the Polish Ministry of Science and Higher Education through the project ‘‘Iuventus Plus’’ (Contract No. 0131/H03/2010/70) and by the National Science Centre through the postdoctoral internship award (Decision No. DEC-2012/04/S/ST9/00020), M.K. was supported by the National Science Centre through the PRELUDIUM funding scheme (Decision No. DEC-2012/05/N/ST9/03857) and M.S. was supported by the National Science Centre through the OPUS 5 funding scheme (Decision No. DEC-2013/09/B/ST2/03455).

Appendix A: Linearized solutions in the vicinity of the de Sitter state

Here we present complete form of the linearized solutions of the system (9) in the vicinity of the de Sitter state. In the case of purely real eigenvalues (model 1a and model 1b) using substitution

$$\frac{\delta}{3 + 2\omega_{\text{BD}}} = \frac{4}{9}n(n-3), \quad (\text{A1})$$

the eigenvalues of the linearization matrix take the following form

$$l_1 = -3, \quad l_2 = -n, \quad l_3 = -3 + n, \quad (\text{A2})$$

and the linearized solutions are

$$\begin{aligned} x(a) = & \frac{4}{\delta}(\Delta x - 2\Delta y) \left(\frac{a}{a^{(i)}} \right)^{-3} + \frac{n}{3\delta(2n-3)} \left(-4n(\Delta x - 2\Delta y) + 3\delta\Delta x - 8(n-3)\Delta\lambda \right) \left(\frac{a}{a^{(i)}} \right)^{-n} + \\ & + \frac{n-3}{3\delta(2n-3)} \left(4(n-3)(\Delta x - 2\Delta y) + 3\delta\Delta x + 8n\Delta\lambda \right) \left(\frac{a}{a^{(i)}} \right)^{-3+n}, \end{aligned} \quad (\text{A3a})$$

$$\begin{aligned} y(a) = & 1 + \frac{1}{2} \left(\frac{4}{\delta} - 1 \right) (\Delta x - 2\Delta y) \left(\frac{a}{a^{(i)}} \right)^{-3} + \frac{n}{6\delta(2n-3)} \left(-4n(\Delta x - 2\Delta y) + 3\delta\Delta x - 8(n-3)\Delta\lambda \right) \left(\frac{a}{a^{(i)}} \right)^{-n} + \\ & + \frac{n-3}{6\delta(2n-3)} \left(4(n-3)(\Delta x - 2\Delta y) + 3\delta\Delta x + 8n\Delta\lambda \right) \left(\frac{a}{a^{(i)}} \right)^{-3+n}, \end{aligned} \quad (\text{A3b})$$

$$\begin{aligned} \lambda(a) = & -2 - \frac{1}{2}(\Delta x - 2\Delta y) \left(\frac{a}{a^{(i)}} \right)^{-3} + \frac{1}{8\delta(2n-3)} \left(-4n(\Delta x - 2\Delta y) + 3\delta\Delta x - 8(n-3)\Delta\lambda \right) \left(\frac{a}{a^{(i)}} \right)^{-n} + \\ & + \frac{1}{8\delta(2n-3)} \left(4(n-3)(\Delta x - 2\Delta y) + 3\delta\Delta x + 8n\Delta\lambda \right) \left(\frac{a}{a^{(i)}} \right)^{-3+n}, \end{aligned} \quad (\text{A3c})$$

where $\Delta x = x^{(i)}$, $\Delta y = y^{(i)} - 1$, and $\Delta\lambda = \lambda^{(i)} + 2$ are the initial conditions.

In the case of the eigenvalues with non-zero imaginary part (model 2) using the substitution

$$\frac{\delta}{3 + 2\omega_{\text{BD}}} = -\frac{1}{9}(9 + 4n^2), \quad (\text{A4})$$

the eigenvalues of the linearization matrix take the following form

$$l_1 = -3, \quad l_2 = -\frac{3}{2} - \mathfrak{i}n, \quad l_3 = -\frac{3}{2} + \mathfrak{i}n, \quad (\text{A5})$$

and the linearized solutions are

$$\begin{aligned} x(a) = & \frac{4}{\delta}(\Delta x - 2\Delta y) \left(\frac{a}{a^{(i)}} \right)^{-3} + \left(-\frac{4}{\delta}(\Delta x - 2\Delta y) + \Delta x \right) \left(\frac{a}{a^{(i)}} \right)^{-3/2} \cos \left(n \ln \left(\frac{a}{a^{(i)}} \right) \right) + \\ & + \frac{1}{6n} \left(-\frac{2}{\delta}(4n^2 - 9)(\Delta x - 2\Delta y) - 9\Delta x - \frac{4}{\delta}(4n^2 + 9)\Delta\lambda \right) \left(\frac{a}{a^{(i)}} \right)^{-3/2} \sin \left(n \ln \left(\frac{a}{a^{(i)}} \right) \right), \end{aligned} \quad (\text{A6a})$$

$$\begin{aligned} y(a) = & 1 + \frac{1}{2} \left(\frac{4}{\delta} - 1 \right) (\Delta x - 2\Delta y) \left(\frac{a}{a^{(i)}} \right)^{-3} + \frac{1}{2} \left(-\frac{4}{\delta}(\Delta x - 2\Delta y) + \Delta x \right) \left(\frac{a}{a^{(i)}} \right)^{-3/2} \cos \left(n \ln \left(\frac{a}{a^{(i)}} \right) \right) + \\ & + \frac{1}{12n} \left(-\frac{2}{\delta}(4n^2 - 9)(\Delta x - 2\Delta y) - 9\Delta x - \frac{4}{\delta}(4n^2 + 9)\Delta\lambda \right) \left(\frac{a}{a^{(i)}} \right)^{-3/2} \sin \left(n \ln \left(\frac{a}{a^{(i)}} \right) \right), \end{aligned} \quad (\text{A6b})$$

$$\begin{aligned} \lambda(a) = & -2 - \frac{1}{2}(\Delta x - 2\Delta y) \left(\frac{a}{a^{(i)}} \right)^{-3} + \left(\frac{1}{2}(\Delta x - 2\Delta y) + \Delta\lambda \right) \left(\frac{a}{a^{(i)}} \right)^{-3/2} \cos \left(n \ln \left(\frac{a}{a^{(i)}} \right) \right) + \\ & + \frac{3}{2n} \left(-\frac{1}{2}(\Delta x - 2\Delta y) + \frac{\delta}{4}\Delta x + \Delta\lambda \right) \left(\frac{a}{a^{(i)}} \right)^{-3/2} \sin \left(n \ln \left(\frac{a}{a^{(i)}} \right) \right), \end{aligned} \quad (\text{A6c})$$

where again $\Delta x = x^{(i)}$, $\Delta y = y^{(i)} - 1$, and $\Delta\lambda = \lambda^{(i)} + 2$ are the initial conditions.

-
- [1] M. Szydlowski, A. Kurek, and A. Krawiec, Phys. Lett. **B642**, 171 (2006), arXiv:astro-ph/0604327.
- [2] C. Brans and R. Dicke, Phys. Rev. **124**, 925 (1961).
- [3] T. Clifton, P. G. Ferreira, A. Padilla, and C. Skordis, Phys. Rept. **513**, 1 (2012), arXiv:1106.2476 [astro-ph.CO].
- [4] P. Ade *et al.* (Planck Collaboration), (2013), arXiv:1303.5076 [astro-ph.CO].
- [5] C. M. Will, *Theory and Experiment in Gravitational Physics*, revised edition ed. (Cambridge University Press, Cambridge, 1993).
- [6] C. M. Will, Living Rev. Rel. **9**, 3 (2006), arXiv:gr-qc/0510072 [gr-qc].
- [7] B. Bertotti, L. Iess, and P. Tortora, Nature **425**, 374 (2003).
- [8] A. Avilez and C. Skordis, (2013), arXiv:1303.4330 [astro-ph.CO].
- [9] Y.-C. Li, F.-Q. Wu, and X. Chen, Phys. Rev. **D88**, 084053 (2013), arXiv:1305.0055 [astro-ph.CO].
- [10] J. C. Fabris, S. Goncalves, and R. de Sa Ribeiro, Grav. Cosmol. **12**, 49 (2006), arXiv:astro-ph/0510779 [astro-ph].
- [11] V. Faraoni, *Cosmology in Scalar-Tensor Gravity*, Fundamental Theories of Physics, Vol. 139 (Kluwer Academic Publishers, Dordrecht, 2004).
- [12] S. Capozziello and V. Faraoni, *Beyond Einstein Gravity. A Survey of Gravitational Theories for Cosmology and Astrophysics*, Fundamental Theories of Physics, Vol. 170 (Springer, New York, 2011).
- [13] O. Hrycyna and M. Szydlowski, Phys. Rev. **D88**, 064018 (2013), arXiv:1304.3300 [gr-qc].
- [14] O. Hrycyna and M. Szydlowski, JCAP **12**, 016 (2013), arXiv:1310.1961 [gr-qc].
- [15] M. Szydlowski, O. Hrycyna, and A. Stachowski, Int. J. Geom. Meth. Mod. Phys. **11**, 1460012 (2014), arXiv:1308.4069 [gr-qc].
- [16] A. Lewis, “CosmoMC,” <http://cosmologist.info/cosmomc/>.
- [17] A. Lewis and S. Bridle, Phys. Rev. **D66**, 103511 (2002), astro-ph/0205436.
- [18] F. Feroz and M. Hobson, Mon. Not. Roy. Astron. Soc. **384**, 449 (2008), arXiv:0704.3704 [astro-ph].
- [19] F. Feroz, M. Hobson, and M. Bridges, Mon. Not. Roy. Astron. Soc. **398**, 1601 (2009), arXiv:0809.3437 [astro-ph].
- [20] F. Feroz, M. Hobson, E. Cameron, and A. Pettitt, (2013), arXiv:1306.2144 [astro-ph.IM].
- [21] N. Suzuki, D. Rubin, C. Lidman, G. Aldering, R. Amanullah, *et al.* (The Supernova Cosmology Project), Astrophys. J. **746**, 85 (2012), arXiv:1105.3470 [astro-ph.CO].
- [22] R. Jimenez and A. Loeb, Astrophys. J. **573**, 37 (2002), arXiv:astro-ph/0106145 [astro-ph].
- [23] J. Simon, L. Verde, and R. Jimenez, Phys. Rev. **D71**, 123001 (2005), arXiv:astro-ph/0412269 [astro-ph].
- [24] E. Gaztanaga, A. Cabre, and L. Hui, Mon. Not. Roy. Astron. Soc. **399**, 1663 (2009), arXiv:0807.3551 [astro-ph].
- [25] D. Stern, R. Jimenez, L. Verde, M. Kamionkowski, and S. A. Stanford, JCAP **02**, 008 (2010), arXiv:0907.3149 [astro-ph.CO].
- [26] M. Moresco, A. Cimatti, R. Jimenez, L. Pozzetti, G. Zamorani, *et al.*, JCAP **08**, 006 (2012), arXiv:1201.3609 [astro-ph.CO].
- [27] N. G. Busca, T. Delubac, J. Rich, S. Bailey, A. Font-Ribera, *et al.*, Astron. Astrophys. **552**, A96 (2013), arXiv:1211.2616 [astro-ph.CO].
- [28] C. Zhang, H. Zhang, S. Yuan, T.-J. Zhang, and Y.-C. Sun, (2012), arXiv:1207.4541 [astro-ph.CO].
- [29] C. Blake, S. Brough, M. Colless, C. Contreras, W. Couch, *et al.*, Mon. Not. Roy. Astron. Soc. **425**, 405 (2012), arXiv:1204.3674 [astro-ph.CO].
- [30] C.-H. Chuang and Y. Wang, Mon. Not. Roy. Astron. Soc. **435**, 255 (2013), arXiv:1209.0210 [astro-ph.CO].
- [31] L. Anderson, E. Aubourg, S. Bailey, F. Beutler, A. S. Bolton, *et al.*, Mon. Not. Roy. Astron. Soc. **439**, 83 (2014), arXiv:1303.4666 [astro-ph.CO].
- [32] Y. Chen, C.-Q. Geng, S. Cao, Y.-M. Huang, and Z.-H. Zhu, (2013), arXiv:1312.1443 [astro-ph.CO].
- [33] D. J. Eisenstein *et al.* (SDSS Collaboration), Astrophys. J. **633**, 560 (2005), arXiv:astro-ph/0501171.
- [34] W. J. Percival *et al.* (SDSS Collaboration), Mon. Not. Roy. Astron. Soc. **401**, 2148 (2010), arXiv:0907.1660 [astro-ph.CO].
- [35] D. J. Eisenstein *et al.* (SDSS Collaboration), Astron. J. **142**, 72 (2011), arXiv:1101.1529 [astro-ph.IM].
- [36] C. P. Ahn *et al.* (SDSS Collaboration), (2013), arXiv:1307.7735 [astro-ph.IM].
- [37] D. H. Jones, M. A. Read, W. Saunders, M. Colless, T. Jarrett, *et al.*, (2009), arXiv:0903.5451 [astro-ph.CO].
- [38] F. Beutler, C. Blake, M. Colless, D. H. Jones, L. Staveley-Smith, *et al.*, Mon. Not. Roy. Astron. Soc. **416**, 3017 (2011), arXiv:1106.3366 [astro-ph.CO].
- [39] M. J. Drinkwater, R. J. Jurek, C. Blake, D. Woods, K. A. Pimbblet, *et al.*, Mon. Not. Roy. Astron. Soc. **401**, 1429 (2010), arXiv:0911.4246 [astro-ph.CO].
- [40] C. Blake, E. Kazin, F. Beutler, T. Davis, D. Parkinson, *et al.*, Mon. Not. Roy. Astron. Soc. **418**, 1707 (2011), arXiv:1108.2635 [astro-ph.CO].
- [41] C. Blake, T. Davis, G. Poole, D. Parkinson, S. Brough, *et al.*, Mon. Not. Roy. Astron. Soc. **415**, 2892 (2011), arXiv:1105.2862 [astro-ph.CO].
- [42] C. Alcock and B. Paczynski, Nature **281**, 358 (1979).
- [43] C. Blake, K. Glazebrook, T. Davis, S. Brough, M. Colless, *et al.*, Mon. Not. Roy. Astron. Soc. **418**, 1725 (2011), arXiv:1108.2637 [astro-ph.CO].
- [44] G. Schwarz, Annals of Statistics **6**, 461 (1978).
- [45] R. E. Kass and A. E. Raftery, Journal of the American Statistical Association **90**, 773 (1995).
- [46] G. Esposito-Farese and D. Polarski, Phys. Rev. **D63**, 063504 (2001), arXiv:gr-qc/0009034 [gr-qc].
- [47] T. Damour and G. Esposito-Farese,

- Class.Quant.Grav. **9**, 2093 (1992).
- [48] T. Damour and G. Esposito-Farese, Phys.Rev. **D53**, 5541 (1996), arXiv:gr-qc/9506063 [gr-qc].
 - [49] B. Greene, K. Hinterbichler, S. Judes, and M. K. Parikh, Phys.Lett. **B697**, 178 (2011), arXiv:0911.0693 [hep-th].
 - [50] M. P. Dabrowski, T. Denkiewicz, and D. Blaschke, Annalen Phys. **16**, 237 (2007), arXiv:hep-th/0507068 [hep-th].
 - [51] V. Faraoni, Class.Quant.Grav. **26**, 145014 (2009), arXiv:0906.1901 [gr-qc].
 - [52] J. A. Frieman, C. T. Hill, A. Stebbins, and I. Waga, Phys.Rev.Lett. **75**, 2077 (1995), arXiv:astro-ph/9505060 [astro-ph].
 - [53] L. Amendola and R. Barbieri, Phys.Lett. **B642**, 192 (2006), arXiv:hep-ph/0509257 [hep-ph].